antibodies produced by wild-type littermates. When immunized with various T cell–dependent antigens, the mutant and wild-type mice produce equal concentrations of specific antibodies that bear the κ chain. Furthermore, antigen-specific B cells homozygous for the $C_\kappa R$ mutation undergo affinity maturation through somatic hypermutation to the same extent as documented for the wild-type C_κ gene. These mutant mice are now waiting to be crossed with animals bearing an analogous replacement mutation in the H chain locus.

REFERENCES AND NOTES

1. J. C. Roder, S. P. C. Cole, D. Kozbor, *Methods Enzymol.* **121**, 140 (1986); C. A. K. Borrebaeck, *Immunol. Today* **9**, 335 (1988).
2. M. S. Neuberger *et al.*, *Nature* **314**, 268 (1985); S. L. Morrison, M. J. Johnson, L. A. Herzenberg, V. T. Oi, *Proc. Natl. Acad. Sci. U.S.A.* **81**, 6851 (1984); P. T. Jones, P. H. Dear, J. Foote, M. S. Neuberger, G. Winter, *Nature* **321**, 522 (1986); L. Riechmann, M. Clark, H. Waldmann, G. Winter, *ibid.* **332**, 323 (1988); M. Verhoeyen, C. Milstein, G. Winter, *Science* **239**, 1534 (1988); C. Queen *et al.*, *Proc. Natl. Acad. Sci. U.S.A.* **86**, 10029 (1989).
3. W. D. Huse *et al.*, *Science* **246**, 1275 (1989); E. Söderland, A. C. Simonsson, C. A. K. Borrebaeck, *Immunol. Rev.* **130**, 109 (1992); A. D. Griffiths, *Curr. Opin. Immunol.* **5**, 263 (1993); I. Lubin *et al.*, *Science* **252**, 427 (1991).
4. M. Brüggemann *et al.*, *Proc. Natl. Acad. Sci. U.S.A.* **86**, 6709 (1989); M. Brüggemann *et al.*, *Eur. J. Immunol.* **21**, 1323 (1991); T. K. Choi *et al.*, *Nature Genet.* **4**, 17 (1993); L. D. Taylor *et al.*, *Nucleic Acids Res.* **20**, 6287 (1992).
5. N. K. Jerne, *Eur. J. Immunol.* **1**, 1 (1971); K. Rajewsky and T. Takemori, *Annu. Rev. Immunol.* **1**, 569 (1983); M. Brüggemann, G. Winter, H. Waldmann, M. Neuberger, *J. Exp. Med.* **170**, 2153 (1989).
6. R. Kühn, K. Rajewsky, W. Müller, *Science* **254**, 707 (1991).
7. Y.-R. Zou, unpublished results.
8. Y.-R. Zou, S. Takeda, K. Rajewsky, *EMBO J.* **12**, 811 (1993).
9. C. Kocks and K. Rajewsky, *Annu. Rev. Immunol.* **7**, 537 (1989).
10. M. L. Rose, M. S. C. Birbeck, V. J. Wallis, J. A. Forrester, A. J. S. Davies, *Nature* **284**, 364 (1980); C. E. Butcher *et al.*, *J. Immunol.* **129**, 2698 (1982); R. F. Coico, B. S. Bhogal, G. J. Thorbecke, *ibid.* **131**, 2254 (1983); M. Apel and C. Berek, *Int. Immunol.* **2**, 813 (1990).
11. I. Förster, P. Vieira, K. Rajewsky, *Int. Immunol.* **1**, 321 (1989).
12. G. M. Griffiths, C. Berek, M. Kaartinen, C. Milstein, *Nature* **312**, 271 (1984).
13. C. Berek, A. Berger, M. Apel, *Cell* **67**, 1121 (1991).
14. H. G. Klobeck, G. Combriato, H. G. Zachau, *Nucleic Acids Res.* **12**, 6995 (1984); P. A. Hieter, E. E. Max, J. G. Seidman, J. V. Meizel Jr., P. Leder, *Cell* **22**, 197 (1980).
15. Plastic plates were coated with CG, KLH, phOX–bovine serum albumin (BSA), or PC-BSA (10 μg/ml), respectively. Diluted serum samples were added, and bound antibodies were detected by biotinylated antibodies for the determination of mouse κ and human κ chains, IgM, and for total IgG. The relative concentration of OX-specific IgG or PC-specific IgM was determined by comparison to standard monoclonal OX- or PC-specific antibodies of the same isotypes. The relative concentrations of CG- or OX-specific κ bearing–antibodies as well as KLH-binding IgM or IgG are shown in Fig. 4 as arbitrary units defined by taking the value of the serum from a pre-immune normal or mutant animal as 1 unit.
16. Total cellular RNA was prepared from 1.8×10^5 PNA^{hi} splenic B cells by as described [H. Gu, I. Förster, K. Rajewsky, *EMBO J.* **9**, 2133 (1990)]. Complementary DNA was synthesized with the Super Script Reverse Transcriptase Kit (BRL). $V_\kappa OX1\text{-}J_\kappa 5$ joints were then amplified with synthesis primers carrying the cloning sites of Bam HI and Hind III ($V_\kappa OX1\text{-}J_\kappa 5$ leader sequence specific primer: TGCGGATCCTCAGTCATAATATCCAG; $J_\kappa 5$ primer: CGGAATTCTTTCAGCTCCAGCTTGG). PCR was performed for 35 cycles. Each cycle consisted of 1 min at 94°C, 1 min at 60°C, and 1 min at 74°C. Amplified L chain fragments were cloned into the PTZ19R vector (Pharmacia).
17. M. Kaartinen, E. Pelkonen, J. Even, O. Mäkelä, *Eur. J. Immunol.* **18**, 1095 (1988).
18. E. A. Kabat, T. Wu, M. Reid-Miller, H. M. Perry, K. S. Gottesman, *Sequences of Proteins of Immunological Interest* (Government Printing Office, Bethesda, MD, 1987).

19. We thank R. Torres and R. Rickert for critical reading of the manuscript; D. Kitamura, R. Kuhn, S. Taki, and W. Muller for advice and discussion; H. G. Zachau for kindly providing the plasmid containing the human C_κ gene; O. Mäkelä, S. Taki, C. Uthoff-Hachenberg, and I. Wolowczuk for antigens and standard antibodies; C. Göttlinger for technical assistance; and U. Ringeisen for the preparation of the figures. The work with animals was conducted in accordance with official regulations. Supported by the Fazit Foundation, the Deutsche Forschungsgemeinschaft through SFB 243, and by the Human Frontier Science Program.

9 August 1993; accepted 1 October 1993

Bcl-2 Inhibition of Neural Death: Decreased Generation of Reactive Oxygen Species

Darci J. Kane,* Theodore A. Sarafian,* Rein Anton, Hejin Hahn, Edith Butler Gralla, Joan Selverstone Valentine, Tõnis Örd, Dale E. Bredesen†

The proto-oncogene *bcl-2* inhibits apoptotic and necrotic neural cell death. Expression of Bcl-2 in the GT1-7 neural cell line prevented death as a result of glutathione depletion. Intracellular reactive oxygen species and lipid peroxides rose rapidly in control cells depleted of glutathione, whereas cells expressing Bcl-2 displayed a blunted increase and complete survival. Modulation of the increase in reactive oxygen species influenced the degree of cell death. Yeast mutants null for superoxide dismutase were partially rescued by expression of Bcl-2. Thus, Bcl-2 prevents cell death by decreasing the net cellular generation of reactive oxygen species.

Expression of Bcl-2 inhibits apoptosis induced by Ca^{2+} ionophores without altering intracellular free Ca^{2+} (*1*), suggesting that Bcl-2 inhibits the cellular death program at a point distal to the rise in intracellular free Ca^{2+}. Apoptosis induced by serum deprivation is not associated with a change in intracellular free Ca^{2+} before the onset of internucleosomal DNA degradation (*1*). The lack of correlation between intracellular free Ca^{2+} and cell death in these studies, along with the similarity of Bcl-2–expressing cells to control cells with respect to morphology, differentiation, growth rate, oxygen consumption, and adenosine triphosphate concentrations (*1*, *2*), prompted a search for a cellular parameter that would explain the resistance of Bcl-2–expressing cells to death.

D. J. Kane, R. Anton, H. Hahn, T. Örd, Department of Neurology, University of California, Los Angeles, CA 90024.
T. A. Sarafian, Department of Pathology, University of California, Los Angeles, CA 90024.
E. B. Gralla and J. S. Valentine, Department of Chemistry and Biochemistry, University of California, Los Angeles, CA 90024.
D. E. Bredesen, Department of Neurology, Brain Research Institute, and the Molecular Biology Institute, University of California, Los Angeles, CA 90024.

*These authors contributed equally to this study.
†To whom correspondence should be addressed at University of California, Los Angeles, CA 90024–1769.

The hypothalamic neural cell line GT1-7 (*3*) displayed a remarkable sensitivity to toxicity from buthionine sulfoximine (BSO), which was abrogated by the expression of Bcl-2. BSO is a specific and essentially irreversible inhibitor of γ-glutamylcysteine synthetase (*4*) and thus decreases the intracellular concentration of reduced glutathione (GSH), a tripeptide involved in protecting the cell from oxidative injury. Although Bcl-2 inhibits apoptosis, the death of GT1-7 cells induced by GSH depletion is necrotic (*5*). This finding argues that Bcl-2 does not inhibit apoptosis per se; rather, Bcl-2 inhibits a cellular process that may result in apoptosis or necrosis.

Treatment of GT1-7 cells with BSO led to cell death within 40 hours, with an LD_{50} (median lethal dose) of ~100 μM (Fig. 1). Stable expression of Bcl-2 by means of a retroviral vector raised the LD_{50} about three orders of magnitude, to greater than 50 mM (Fig. 1). Measurement of intracellular GSH with monochlorobimane (MCB, Molecular Probes) (*6*) confirmed a decrement after exposure to BSO for both control and Bcl-2–expressing cells (Fig. 2A). However, cells expressing Bcl-2 had two to three times the basal concentrations of GSH and correspondingly higher concen-

trations during BSO treatment (Fig. 2A). To determine whether the survival of neural cells expressing Bcl-2 was a result of the increase in GSH, we used diethyl maleate to bind the free sulfhydryl groups of GSH (*7*). After exposure to 1 mM diethyl maleate, cells expressing Bcl-2, as well as control cells, had a decrease of more than 90% in GSH (Fig. 2A). Despite this, cells expressing Bcl-2 survived (Fig. 2, B and C), demonstrating that the increase in survival of Bcl-2–expressing cells is not simply a result of the increase in total cellular GSH. Because neither diethyl maleate nor BSO rapidly depletes mitochondrial GSH (*8*), cells were treated with ethacrynic acid, which depletes both cytosolic and mitochondrial GSH (*9*). Treatment of GT1-7 cells with 200 μM ethacrynic acid resulted in the death of control cells within 24 hours, but Bcl-2–expressing cells remained viable (*10*).

Because the elevated GSH associated with Bcl-2 might have resulted from decreased utilization of GSH, the fluorescent probe dichlorofluorescein diacetate (DCF) (*11*) was used to measure the net intracellular generation of reactive oxygen species in diethyl maleate–treated cells to determine whether Bcl-2 effected a decrement in oxidative stress. This probe measures primarily hydrogen peroxide and hydroxyl radical (*11*). By 90 min the DCF fluorescence of control cells had increased by a factor of 23 (Fig. 3); cells died between 2 and 3 hours (Fig. 2C). In contrast, the Bcl-2–expressing cells showed only a modest increase in DCF fluorescence (Fig. 3) and the cells survived (Fig. 2C). Similar results were obtained with ethacrynic acid treatment. To distinguish between a causal and noncausal association of neural cell death with reactive oxygen species in this system, we manipulated the concentration of reactive oxygen species with various compounds in conjunction with diethyl maleate and examined the effect on GT1-7 viability. The addition of the iron chelator desferrioxamine (100 μM) (*12*) reduced reactive oxygen species production (Fig. 4A) as well as inhibited cell death induced by GSH depletion (Fig. 4B). The antioxidants ascorbic acid (1 mM) and *N*,*N*′-diphenyl-*p*-phenylenediamine (25 μM) (*13*) inhibited the BSO-induced death of control GT1-7 cells (Fig. 2B) and reduced reactive oxygen species (Fig. 4A). When aminotriazole was used to inhibit catalase (*13*) simultaneously with GSH depletion, control cells demonstrated a rise in reactive oxygen species above that associated with GSH depletion alone (Fig. 4A). Correspondingly, control cells died more quickly than cells that had only been depleted of GSH (Fig. 4B).

The diminished net cellular generation of reactive oxygen species in Bcl-2–expressing GT1-7 cells depleted of GSH was associated with an inhibition of lipid peroxidation: whereas lipid peroxidation in control cells treated with 1 mM diethyl maleate increased after 2 hours (prior to cell death), no increase in lipid peroxidation occurred in cells expressing Bcl-2 (Fig. 5).

To exclude the possibility of the involvement of nitric oxide, we tested the effect of inhibited nitric oxide synthesis with nitro-L-arginine methyl ester (300 μM) (*14*) and the effect of enhanced nitric oxide production induced by *S*-nitroso-*N*-acetylpenicillamine (1 μM) (*15*). In neither case was there a difference between control cells and Bcl-2–expressing cells with respect to reactive oxygen species production or cell death (*16*).

The hypothesis that the expression of Bcl-2 inhibits cell death by decreasing the net cellular generation of reactive oxygen species predicts that Bcl-2 expression should enhance the growth of cells deficient in superoxide dismutase. Therefore, mutants of the yeast *Saccharomyces cerevisiae* that carry null mutations for copper-zinc superoxide dismutase (*sod1*) or manganese superoxide dismutase (*sod2*) were transformed with an expression construct for Bcl-2 or a control construct lacking the coding sequence for Bcl-2. As demonstrated previously, *sod2* mutants grew poorly under conditions of respiratory metabolism, whereas wild-type *S. cerevisiae* grew well

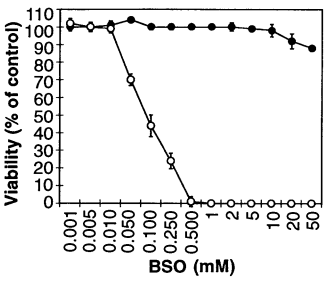

Fig. 1. Neural cell death in response to BSO. Solid circles, GT1-7 cells expressing Bcl-2; open circles, control cells lacking Bcl-2 expression. Each data point shows the mean of quadruplicate cultures with standard deviations. The experiment was performed six times. Error bars of less than 2% are embedded in the symbols. GT1-7 cells were infected with a recombinant retrovirus (pBP–*bcl-2*) or a control retrovirus, both constructed and infected as described (*2*). Immunocytochemistry demonstrated that >98% of the selected cells expressed Bcl-2, whereas the control cells did not express Bcl-2. Cells were plated at a density of 10^5 cells per well in poly-L-lysine–coated 96-well tissue culture plates (Costar) in Dulbecco's modified Eagle's medium (DMEM) with 10% fetal bovine serum. The L-buthionine-[S,R]-sulfoximine (Sigma) was dissolved in medium to make a 100 mM stock. BSO was added at the concentrations indicated, incubated for 24 hours, then removed and replaced by fresh medium. Cell viability was determined 24 hours later by formazan production from diphenyltetrazolium salt (MTT assay, as modified by Hansen *et al.*) (*20*).

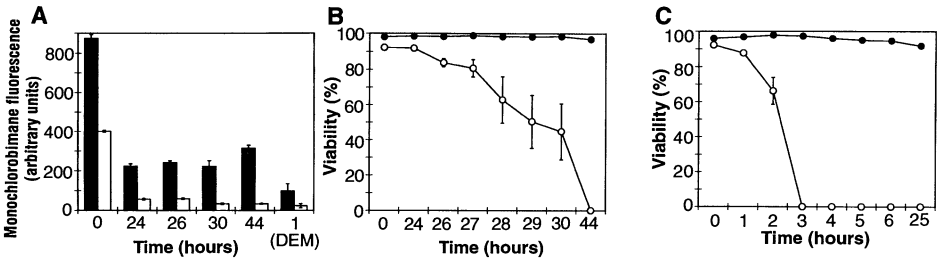

Fig. 2. (**A**) Cellular GSH in GT1-7 cells is increased in association with Bcl-2 expression (solid bars) and falls during treatment with BSO or diethyl maleate (DEM). Bars show quantitated fluorescence of cells incubated with MCB, which fluoresces in the presence of GSH (*6*). Data shown represent the average of quadruplicate cultures, and the experiment was repeated three times. Unfilled bars, control cells (GT1-7 lacking Bcl-2 expression). Cells were assayed for GSH before BSO exposure (t = 0), then exposed to 500 μM BSO for 24 hours, after which the medium was replaced with fresh medium, and GSH was again assayed (t = 24 hours). Over the next several hours GSH was assayed until the control cells had died. Also shown are the GSH concentrations of cells treated with 1 mM DEM for 1 hour. (**B**) Viability of GT1-7 cells lacking Bcl-2 expression (open circles) falls quickly after exposure to BSO for 24 hours. Viability of cells expressing Bcl-2 (solid circles) remained high throughout the experiment. Each data point represents the average of quadruplicate cultures, with standard deviations shown (error bars of less than 2% are embedded in the symbols). The experiment was performed three times. (**C**) Viability of GT1-7 cells lacking Bcl-2 expression (open circles) falls very quickly after treatment for 1 hour with 1 mM DEM at 23°C, whereas cells expressing Bcl-2 (closed circles) remained viable after a reduction in GSH to less than 10% of their original concentration. Cellular GSH was measured with MCB (*6*). MCB (40 μM) was added to cells in 96-well plates and the cells incubated for 15 min, then fluorescence at 460 nm in response to excitation at 395 nm was quantitated with a Cytofluor 2300 plate reader (Millipore, Inc.). Cell death was quantitated by propidium iodide fluorescence (emission at 590 nm in response to excitation at 530 nm). Propidium iodide (Aldrich) was prepared as a 5 mM stock in water, diluted to 20 μM in medium, and added to cells, and fluorescence was read after 15 min of incubation. Total cell numbers were confirmed by Hoechst 33342 staining as described (*21*).

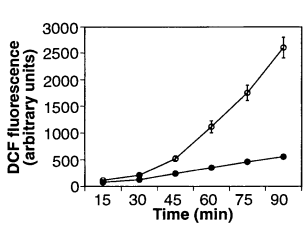

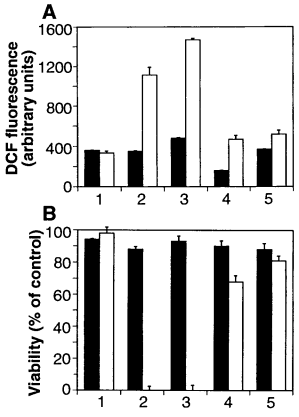

Fig. 3 (left). Intracellular generation of reactive oxygen species in GT1-7 cells expressing Bcl-2 (solid circles) or control transfectants (open circles) treated with 1 mM DEM. Cells were plated at a density of 10^5 cells per well in a 96-well tissue culture plate (Nunc) that had been coated with poly-L-lysine (Sigma). Wells were washed three times with a modified Krebs-Ringer solution (KR, 20 mM Hepes, 10 mM dextrose, 127 mM NaCl, 5.5 mM KCl, 1 mM $CaCl_2$, and 2 mM $MgSO_4$, pH 7.4), then KR buffer containing DCF (1 μg/ml) (Molecular Probes) plus 1 mM DEM (Sigma) was added in a total volume of 100 μl. Plates were read on a Cytofluor 2300 plate reader, with an excitation wavelength of 485 nm and an emission wavelength of 530 nm, at 15-min intervals for 90 min. Each point represents the average of triplicate wells with error bars included. This experiment was repeated six times with reproducible results; the one shown is representative. Error bars representing less than 50 DCF fluorescence units are embedded in the symbols. **Fig. 4 (right).** (**A**) Modulation of intracellular generation of reactive oxygen species. Cells were treated as described in Fig. 3, but with the addition of either (bar 1) KR and DCF only; (bar 2) KR and DCF plus 1 mM DEM; (bar 3) KR, DCF, and DEM plus 25 mM aminotriazole (Sigma); (bar 4) KR, DCF, and DEM plus 100 μM desferrioxamine mesylate (Sigma); or (bar 5) KR, DCF, and DEM plus 1 mM ascorbic acid (Sigma). (Similar results were obtained with 25 μM diphenyl-*p*-phenylenediamine.) KR, modified Krebs-Ringer as described in Fig. 3; DCF (1 μg/ml). The bars represent the fluorescence recorded 60 min after the addition of diethyl maleate, DCF, and the various compounds. Each experiment was performed at least two times, and the data shown represent the average of triplicate wells with error bars included. Filled bars, Bcl-2–expressing cells; unfilled bars, control transfectants. (**B**) Viability of Bcl-2–expressing cells compared with control transfectants in response to various agents. Cells were plated at a density of 10^5 cells per well in poly-L-lysine–coated 96-well plates (Nunc), then grown in high glucose (4.5 g/liter) DMEM plus 10% heat-inactivated fetal bovine serum in a 37°C humidified incubator in 5% CO_2 and 95% air. After allowing the cells to adhere overnight, we removed the culture medium and replaced it with medium containing either (bar 1) 500 μM BSO, assayed after 24 hours; (bar 2) 500 μM BSO, assayed after 48 hours; (bar 3) 500 μM BSO plus 25 mM aminotriazole, assayed after 24 hours; (bar 4) 500 μM BSO plus 100 μM desferrioxamine mesylate, assayed after 48 hours; or (bar 5) 500 μM BSO plus 1 mM ascorbic acid, assayed after 48 hours. (Similar results were obtained with 25 μM diphenyl-*p*-phenylenediamine.) Viability was determined either 24 or 48 hours later, as indicated, by two methods: the MTT assay (*20*), which reflects the number of viable cells, and by quantitation of propidium iodide fluorescence, as a measure of cell death. For the fluorescence assay, we confirmed total cell numbers by lysing the cells with 50 μM digitonin, then adding propidium iodide (20 μg/ml); 15 min later, fluorescence was quantitated with a Cytofluor 2300 plate reader, with an excitation wavelength of 530 nm and an emission wavelength of 645 nm. Data generated by both assays were in good agreement and representative data are shown here. Data shown represent the average of triplicate wells with standard errors shown, and each experiment was performed at least two times. Filled bars, Bcl-2–expressing cells; unfilled bars, control cells.

under these conditions (*17*). Bcl-2 expression enhanced the growth of *sod2* mutants that were grown in 21% oxygen under conditions requiring respiratory metabolism, and to a lesser extent, Bcl-2 expression enhanced the growth of *sod1* mutants in fermentative conditions (*18*). However, Bcl-2 expression did not increase superoxide dismutase activity in the yeast mutants nor enhance the growth of a histidine auxotroph (*18*).

The involvement of iron [indicated by the protective effect of a concentration of desferrioxamine that has iron-binding but not radical-scavenging properties (100 μM)] (*12*) and hydrogen peroxide (indicated by the effect of catalase inhibition) suggests the possibility that hydroxyl radicals might mediate neural cell death in this system. Bcl-2 expression may decrease the generation or increase the scavenging of reactive oxygen species. The lack of effect of nitro-L-arginine methyl ester and *S*-nitroso-*N*-acetylpenicillamine suggests that, at least in this system, nitric oxide is not the most important mediator of cell death that is inhibited by Bcl-2 expression.

Several mechanisms for the observed inhibition of the net cellular generation of reactive oxygen species by Bcl-2 would be compatible with these data: (i) Bcl-2 may function as a direct radical-scavenging protein, (ii) Bcl-2 may be a metal-binding protein, or (iii) Bcl-2 may inhibit the transfer of electrons from complexes I through III to dioxygen in the mitochondrial inner membrane, thus decreasing the formation of superoxide. Any of these models would be compatible with the finding that Bcl-2 inhibits apoptosis in cells devoid of functional mitochondrial DNA (*19*). This is because extramitochondrial generation of free-radical species represents a significant contribution to the overall cellular generation of such species (*17*) and cells lacking functional mitochondrial DNA nevertheless generate reducing equivalents and have incomplete respiratory complexes I, III, and IV (and a complete complex II), making it likely that these cells do generate reactive oxygen species.

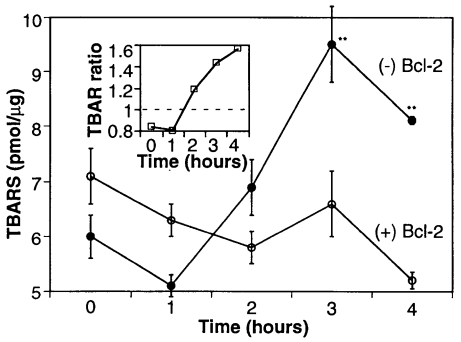

Fig. 5. Expression of Bcl-2 prevents lipid peroxidation after GSH depletion. GT1-7 cells were maintained as described in Fig. 1. After the cells were treated with DEM (1 mM) at 37°C, we assessed lipid peroxidation by determining the quantity of thiobarbituric acid–reactive substances (TBARS) as a measure of malondialdehyde formation (*22*). A Cytofluor 2300 plate reader was used to measure fluorescence at 590 nm, with an excitation wavelength of 530 nm. Standard curves were prepared with tetraethoxypropane as a lipoperoxide standard and immunoglobulin as a protein standard. At t = 0, 1, and 2 hours no significant differences in TBARS per microgram of protein were detected between control and Bcl-2–expressing cells, but at t = 3 and 4 hours, highly significant differences occurred. (P <0.0001 by two-way analysis of variance, n = 14; indicated by asterisks), both between control and Bcl-2–expressing cells and between control (at t = 0) and control (at t = 3 and 4 hours). The increase in TBARS in control cells preceded cell death, which was 7 ± 1% at t = 3 hours and 30 ± 3% at t = 4 hours, determined with propidium iodide as in Fig. 2. At no time point did the cells expressing Bcl-2 demonstrate a significant rise in thiobarbituric acid–reactive substances in comparison with the value at t = 0. (**Inset**) Ratio of thiobarbituric acid–reactive substances (picomoles per microgram of protein) present in control cells to those present in Bcl-2–expressing cells at t = 0 to 4 hours, demonstrating a progressive increase.

REFERENCES AND NOTES

1. L. Zhong *et al.*, *Proc. Natl. Acad. Sci. U.S.A.* **90**, 4533 (1993).
2. S. P. Mah *et al.*, *J. Neurochem.* **60**, 1183 (1993).
3. P. L. Mellon *et al.*, *Neuron* **5**, 1 (1990).
4. O. W. Griffith, *J. Biol. Chem.* **257**, 13704 (1982).
5. D. J. Kane, T. Örd, R. Anton, D. E. Bredesen, in preparation.
6. D. C. Shrieve, E. A Bump, G. C. Rise, *J. Biol. Chem.* **263**, 14107 (1988). There is a linear relation between the MCB fluorescence intensity and the intracellular concentration of GSH

7. R. H. Ku and R. E. Billings, *Arch. Biochem. Biophys.* **247**, 183 (1986).
8. O. W. Griffith and A. Meister, *Proc. Natl. Acad. Sci. U.S.A.* **82**, 4668 (1985).
9. M. J. Meredith and D. J. Reed, *J. Biol. Chem.* **257**, 3747 (1982).
10. D. J. Kane *et al.*, unpublished data.
11. A. R. Rosenkranz *et al.*, *J. Immunol. Methods* **156**, 39 (1992).
12. I. Morel *et al.*, *Free Radical Biol. Med.* **13**, 499 (1992).
13. P. E. Starke and J. L. Farber, *J. Biol. Chem.* **260**, 86 (1985).
14. R. G. Kilbourn *et al.*, *Biochem. Biophys. Res. Commun.* **172**, 1132 (1990).
15. U. C. Garg and A. Hassid, *J. Clin. Invest.* **83**, 1774 (1989).
16. D. J. Kane *et al.*, unpublished data.
17. E. B. Gralla and D. J. Kosman, *Adv. Gen.* **30**, 251 (1992).
18. An 850–base pair (bp) fragment containing the open reading frame of the human *bcl-2* complementary DNA (cDNA) was ligated into the expression vector pAD4 containing the strong promoter of the alcohol dehydrogenase gene and the LEU2 selectable marker, and this construct was used for transformation of yeast. A vector without the 850-bp *bcl-2* fragment was used as a control. Four strains of yeast were transformed with the two constructs: the parental strain (DBY746; **α**, *leu2-3, 11 his3Δ1 trp1-298a ura3-52*); *sod1* (EG118; **α**, *leu2-3, 11 his3Δ1 trp1-298a ura3-52*; *sod1ΔA::URA3*); *sod2* (EG110; **α**, *leu2-3, 11 his3Δ1 trp1-298a ura3-52*; *sod2Δ::TRP1*); and *sod1sod2* (EG133; **α**, *leu2-3, 11 his3Δ1 trp1-298a ura3-52*; *sod1ΔA::URA3 sod2Δ::TRP1*). The lithium acetate method was used for transformation (*23*). After transformation and selection in medium lacking leucine, yeast were quantified by an assay of the optical density at 600 nm, then equal numbers were streaked in each of six plate sections and grown for 5 days in room air or in an atmosphere of 100% O_2. As a control, Bcl-2 was expressed in a histidine auxotroph; no growth was detected on His^- plates. Enhanced growth of *sod2* mutants expressing Bcl-2 was demonstrated by (i) growth on glycerol plates in 21% oxygen (no growth detected for pAD4-transformed *sod2* mutants) and (ii) enhanced plating efficiency on glycerol in 21% oxygen (0 for pAD4 control compared with 4×10^3 for Bcl-2–expressing *sod2* mutants and 5×10^5 for wild-type *S. cerevisiae*). Enhanced growth of *sod1* mutants expressing Bcl-2 was demonstrated by (i) growth on dextrose in reduced (~10%) oxygen (no growth detected for pAD4-transformed *sod1* mutants) and (ii) increased growth in liquid culture; optical densities were compared for *sod1* mutants transformed with pAD4 with those transformed with pAD4–*bcl-2*. After 6 hours in culture, the optical density of the pAD4-transformed *sod1* mutants was 4.4, in comparison with 7.2 for those transformed with pAD4–*bcl-2*.
19. M. D. Jacobson *et al.*, *Nature* **361**, 365 (1993).
20. M. B. Hansen, S. E. Nielsen, K. Berg, *J. Immunol. Methods* **119**, 203 (1989).
21. W. L. Richards *et al.*, *Exp. Cell Res.* **159**, 235 (1985).
22. K. Yagi, *Biochem. Med.* **15**, 212 (1976).
23. H. Ito, Y. Fukuda, K. Murata, A. Kimura, *J. Bacteriol.* **153**, 163 (1983).
24. We thank M. Cleary for the *bcl-2* cDNA; P. Mellon for the GT1-7 cells; J. Colicelli for the pAD4 yeast expression vector; H. Land for the pBabe expression vector; L. Ignarro for the nitro-L-arginine methyl ester and *S*-nitroso-*N*-acetylpenicillamine; S. Clarke, C. Clarke, R. Weiss, and C. Kayalar for thoughtful discussions; and K. Moghaddami for administrative assistance. Supported by NIH grant NS27812 (D.E.B.), NIH grant GM 28222 (J.S.V.), and a Margaret E. Early Medical Research Trust grant (E.B.G.).

16 July 1993; accepted 15 September 1993

Sensing Structural Intermediates in Bacterial Flagellar Assembly by Export of a Negative Regulator

Kelly T. Hughes,* Karen L. Gillen, Melinda J. Semon, Joyce E. Karlinsey

The ability of a regulatory protein to sense the integrity of the bacterial flagellar structure was investigated. In response to a defective hook–basal body complex, the anti-σ^{28} FlgM protein inhibits flagellin transcription. In cells with a functional hook–basal body complex, the flagellin genes are transcribed normally and the FlgM protein is expelled into the growth medium. In strains with a defective hook–basal body structure, FlgM is absent from the media. The presence of flagellin protein in the media is substantially reduced in strains carrying a FlgM-LacZ protein fusion, suggesting that the fusion is blocking the flagellar export apparatus. These results suggest that the FlgM protein assesses the integrity of the flagellar hook–basal body complex by itself being a substrate for export by the flagellar-specific export apparatus.

In both prokaryotes and eukaryotes, developmental pathways involving the synthesis and assembly of structures often proceed through structural intermediates. The synthesis of the flagellar organelle in bacteria provides a model system to study the coordination of transcriptional regulation with the assembly of structural intermediates. The flagellum is composed of a basal body structure, located in the cell membrane, and an extracellular hook, which acts as a flexible joint to which the flagellar filament is attached (Fig. 1). The genetics and biogenesis of the bacterial flagella have been recently reviewed (*1*). Components of the basal body complex are assembled into a structure that includes a motor driven by a proton pump, a switch complex that determines the direction of flagellar rotation, a rod structure that transverses the two membranes and the cell wall, ring proteins embedded within the membranes that stabilize the structure, and a flagellar-specific export apparatus at the cytoplasmic base. Assembly of the extracellular component of the flagellum involves the transport of individual components through a pore in the basal body structure (*2*). A flagellar-specific export pathway (*3*) determines which proteins are exported by what may be an ordered assembly mechanism (*1*). The hook subunits are exported and assembled to complete the hook–basal body structure, and then the export apparatus is possibly modified to stop the export of hook subunits and begin the export of flagellin subunits to be assembled into the flagellar filament (*4*).

The genes required for flagella synthesis and chemotaxis in the bacterium *Salmonella typhimurium* are organized into a regulatory hierarchy of three classes (*5*). Each class is required for expression of the next. The early class includes two master regulatory genes that respond to global signals such as cAMP (adenosine 3′,5′-monophosphate) levels (*6*, *7*), and when induced they turn

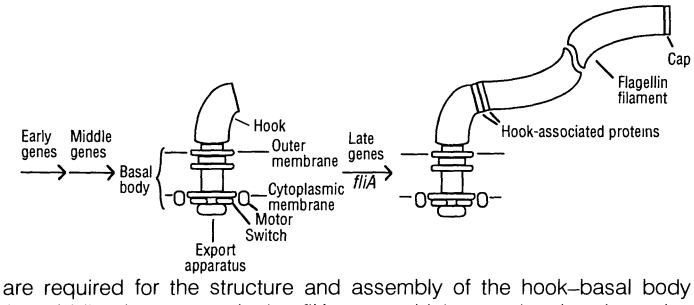

Fig. 1. Biosynthesis of the *S. typhimurium* flagellar structure. The genes required for synthesis of flagella are grouped into three classes (*5*). The early class encodes positive activators required for the expression of the middle class genes. The middle class genes are required for the structure and assembly of the hook–basal body complex (*1*). Included in the middle class genes is the *fliA* gene, which encodes the alternative sigma factor, σ^{28} (*8*). This sigma factor is specific for the transcription of the late class genes, which encode the flagellin filament genes, hook-associated proteins, and the flagellar cap protein. The *flgM* gene is transcribed from both middle and late class promoters (*16*).

Department of Microbiology, SC-42, University of Washington, Seattle, WA 98195.

*To whom correspondence should be addressed.